Bioactive Materials 6 (2021) 1618–1627

Contents lists available at ScienceDirect

Bioactive Materials

journal homepage: www.sciencedirect.com/journal/bioactive-materials

Nitric oxide-generating compound and bio-clickable peptide mimic for synergistically tailoring surface anti-thrombogenic and anti-microbial dual-functions

Han Yu [a], Shaoxing Yu [a], Hua Qiu [a], Peng Gao [a], Yingzhong Chen [b], Xin Zhao [c], Qiufen Tu [a], Minggang Zhou [b,**], Lin Cai [b], Nan Huang [a], Kaiqin Xiong [a,***], Zhilu Yang [a,*]

[a] Key Laboratory of Advanced Technology for Materials of the Education Ministry, School of Materials Science and Engineering, Southwest Jiaotong University, Chengdu, 610031, China
[b] Department of Cardiology, Third People's Hospital of Chengdu Affiliated to Southwest Jiaotong University, Chengdu, 610031, China
[c] Department of Biomedical Engineering, The Hong Kong Polytechnic University, Hung Hom, Hong Kong, China

ARTICLE INFO

Keywords:
Nitric oxide
Bio-clickable peptide mimic
Synergic modification
Anti-thrombosis
Anti-infection

ABSTRACT

Application of extracorporeal circuits and indwelling medical devices has saved many lives. However, it is accompanied with two major complications: thrombosis and infection. To address this issue, we apply therapeutic nitric oxide gas (NO) and antibacterial peptide for synergistically tailoring such devices for surface anti-thrombogenic and antifouling dual functions. Such functional surface is realized by stepwise conjugation of NO-generating compound of 1,4,7,10-tetraazacyclododecane-1,4,7,10-tetraacetic acid (DOTA) chelated copper ions (Cu-DOTA) and dibenzylcyclooctyne- (DBCO-) modified antimicrobial peptide based on carbodiimide and click chemistry respectively. The integration of peptide and Cu-DOTA grants the modified surface the ability to not only efficiently inhibit bacterial growth, but also catalytically generate NO from endogenous *s*-nitrosothiols (RSNO) to reduce adhesion and activation of platelets, preventing the formation of thrombus. We envision that the stepwise synergistic modification strategy by using anticoagulant NO and antibacterial peptide would facilitate the surface multifunctional engineering of extracorporeal circuits and indwelling medical devices, with reduced clinical complications associated with thrombosis and infection.

1. Introduction

Nowadays, the widespread application of blood-contacting devices has saved numerous lives by hemodialysis, nutritional support, drug delivery and extracorporeal circulation [1]. However, the demand for co-administration of antibiotics and anticoagulants in clinic to reduce infections and thrombosis substantially brings out the potential hazards in blood-contacting devices [2]. Besides, these devices' shortcomings such as heparin-induced thrombocytopenia [3] and bacterial resistance [4] potentially caused by drugs, epidermal necrolysis [5], deep phlebitis [6], or catheter-related bloodstream infections [7] are much more life-threatening during cardiopulmonary bypass in practice.

The urgent clinical need of decreasing infection and blood clotting with minimized usage of drugs has stimulated the pursuit for surface modification strategies to provide antibacterial and anticoagulant dual functions. Up to date, the most successful approaches have been active strategies, in which the implanted materials and devices elute drugs (e.g., noble metals [8], heparin [9], antibiotics [10], and peptide [11]) to prevent the activation of platelets or to kill bacteria. Although these available methods have been widely implemented in research, limitations persist because the interaction between blood protein and the material surface is not regulated validly, and the anti-infection and anti-coagulation properties may lose rapidly after drug release [12]. In addition, common surface molecule grafting strategies such as the amide coupling [13] usually provide limited long-term bioactivity due to the probabilistic reaction of multiple chemical groups. Hence, according to the currently underway human clinical evaluation of these surface coatings, there is no benefit compared to clinical practice with heparin

* Corresponding author.
** Corresponding author.
*** Corresponding author.
E-mail addresses: zhoumg1997@163.com (M. Zhou), xkqhe@126.com (K. Xiong), zhiluyang1029@swjtu.edu.cn (Z. Yang).

https://doi.org/10.1016/j.bioactmat.2020.11.011
Received 21 October 2020; Received in revised form 10 November 2020; Accepted 10 November 2020
Available online 23 November 2020

[14,15].

Different from the exogenous devices, the blood vessel possessed excellent antibacterial and anticoagulant properties, which stems from the microenvironment [16] and its physiological activities [17]. Antimicrobial peptide (AMP), as a key component of the immune system, are widely distributed in plasma to kill bacteria directly and recruit lymphocytes to resist infection when wounds occur [18]. It is reported that more than 2000 species of AMP have been isolated from multitudinous sources [19]. It is note-worthy that peptides are not susceptible to bacterial resistance and has wide antimicrobial properties unlike most antibiotics [20]. Although the structural and functional differences are abundant among these AMP, the common properties such as highly cationic character and the amphipathic structures provide areas of interest for surface modification [19]. In addition, endothelial cells release a series of factors, e.g., Nitric oxide (NO) therapeutic gas, into the surrounding microenvironment *in vivo*, which plays a significant role in numerous processes such as up-regulating cyclic guanylate monophosphate (cGMP) expression in platelets to reduce the activation and aggregation, thus preventing the formation of thrombosis [21].

Here, inspired by the healthy blood vessel microenvironment, we combined antithrombotic and antibacterial activities by integrating the NO and antibacterial peptides based on amide coupling and click chemistry (Fig. 1). A highly effective NO catalytic species, Cu-DOTA [22], and a molecular anchor, Azide-NHS were immobilized to the aminated surface in sequence, and the bio-clickable antibacterial peptide, DBCO-AMP, was subsequently tethered to this anchor by click-reaction. The stepwise synergistic modification strategy supported well-maintained molecular configuration/conformation of AMP and

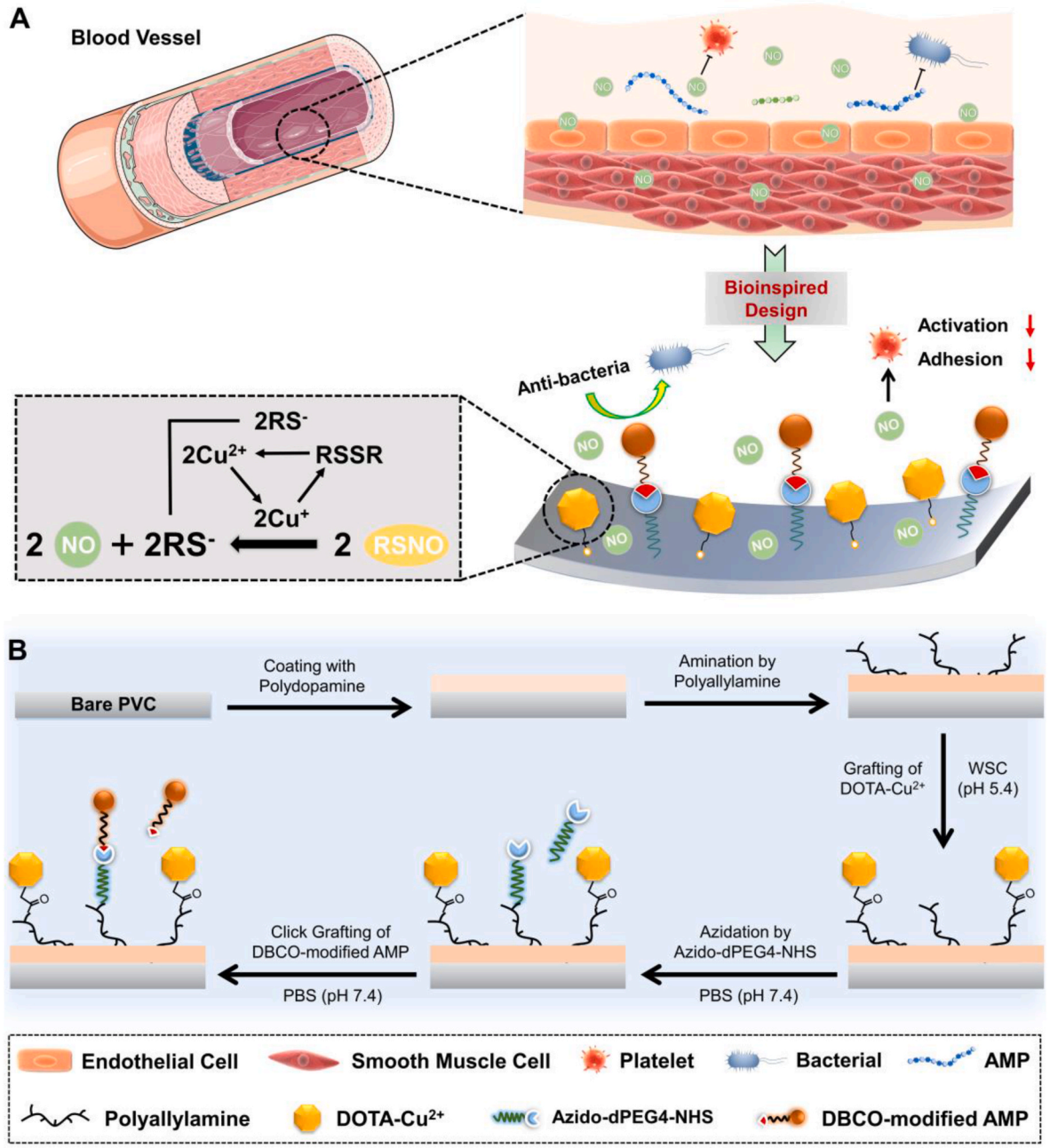

Fig. 1. (A) Bio-inspired design of multifunctional surface with the combination of catalytic release of NO, induced by Cu-DOTA and anti-microbial peptide, which realizes the integration of both antithrombogenic and antifouling properties. (B) Synergistic grafting of Cu-DOTA and anti-microbial peptide based on carbodiimide and click chemistry respectively.

avoided the potential cross-reaction between grafted molecules. We showed that the PVC functionalized by AMP and Cu-DOTA i.e., AMP@Cu-DOTA presented excellent antibacterial efficiency against both *E. coli* and *S. epidermids*. A rabbit *ex vivo* circulation test demonstrated the merit of AMP@Cu-DOTA surface in terms of thrombosis reduction. In a word, these positive results shown in this study provide a new approach for not only multicomponent surface engineering strategy, but also the creation of multifunctional extracorporeal circuits and indwelling medical devices with improved clinical outcomes associated with anti-infection and anti-thrombosis.

2. Materials and methods

2.1. Materials

Copper chloride dehydrate (CuCl2·2H2O), NaOH (Purity ≥ 98.0%), Dimethyl sulfoxide (DMSO), Tri-tert-butyl 1,4,7,10-Tetraazacyclododecane-1,4,7,10-tetraacetate (DOTA, purity ≥ 98.0%), N-(3-dimethylaminepropyl)-N′-ethylcarbodiimide (EDC, purity ≥ 98.0%), N-hydroxysuccinimide (NHS, purity ≥ 97.0%), 2-(N-morpholino) ethanesulfonic acid hydrate (MES, Purity ≥ 97.0%), Tris-HCl (Purity ≥ 97.0%), 1-[(1-Azido-15-oxo-3,6,9,12-tetraoxapentadecan-15-yl) oxy] pyrrolidine-2,5-dione (Azido-dPEG4-NHS), polyallylamine alkaline, Acid Orange II (AO II), phosphatic buffer solution (PBS), S-nitrosoglutathione (GSNO, purity ≥ 97.0%), reduced glutathione (GSH, purity ≥ 97.0%), Cyclic Guanosine Monophosphate (cGMP) and γ-chain fibrinogen ELISA Kits were purchased from Sigma-Aldrich. Peptide ((DBCO-Mal)-(Mpa)-(PEG5)-WFWKWWRRRRR, DBCO-AMP) was synthesized with the assistance of China Peptides Co. Ltd. (Shanghai, China, purity > 95%).

2.2. Preparation of the amine-bearing coating

To fabricate the amine-bearing coating, firstly, the polyvinyl chloride (PVC, one of the most popular materials used for fabricating blood-contacting tubing) substrates (2.5 cm × 2.5 cm) were immersed into dilute aqueous solution of dopamine (1 mg/mL) dissolved in 10 mM tris buffer (pH 8.5). After deposition for 24 h, the polydopamine (PDA)-coated PVC substrates were rinsed by distilled water and dried by a flow of nitrogen gas (N_2). PDA is the lack of surface amine groups. When PDA was treated by an amine-rich polymer, polyallylamine, in alkaline solution, it would finally convert into a coating rich in amine groups that is marked as PADA. This reaction primarily base on the Schiff base reaction or Michael addition. The high density of amine groups on the PADA is beneficial for subsequent immobilizing of molecules with carboxyl groups based on carbodiimide chemistry. To obtain such an amine-bearing PADA coating, subsequently, the PDA-coated PVC substrates mentioned above were immersed into the polyallylamine alkaline solution (pH 12) for amination for 12 h at room temperature. Finally, the obtained amine-bearing PADA-coated PVC was washed by distilled water and dried by N_2.

2.3. Preparation of the AMP@Cu-DOTA coating

DOTA is a kind of cyclones with four carboxyl groups, which can be immobilized on anmie-bearing PADA through the interaction of carboxyl groups and amine groups, that is, amide coupling. Meanwhile, copper ions can be effectively chelated into the center of DOTA, thus form a stable NO catalytically generating species. Here, $CuCl_2{\cdot}2H_2O$ and DOTA (0.1 mg/mL) were firstly mixed in molar ratio of 1:1 in deionized water to prepare the Cu-DOTA coordination complex. Then the Cu-DOTA (0.11 mg/mL) were activated in water-soluble carbodiimide (WSC) solution consisting of EDC (1 mg/mL), NHS (0.24 mg/mL) and MES (9.76 mg/mL) for 30 min in advance. Afterwards, the PADA-modified PVC substrates were immersed into the above reaction system. After grafting for 12 h, the Cu-DOTA-functionalized PVC were washed with PBS and distilled water in sequence, and then dried by N_2 before surface analysis. The immobilization of the Cu-DOTA on PADA just consumption partial of the surface amine groups of PADA by controlling of feed Cu-DOTA concentration and reaction time (this grafting type belong to "carbodiimide chemistry"), then grafted the Azido-dPEG4-NHS by utilizing the rest amine groups. The grafted Azido acted as an anchor for further specifically bonding with DBCO-modified AMP based on "click chemistry". PEG act as a spacer in each synthetic molecule. The spacer is flexible and increased the distance between functional molecular segment and binding site, thus make the grafted molecules with higher activity.

To further grafting AMP, the Cu-DOTA-modified specimens containing the residual amine groups were first Azide-functionalized by carbodiimide chemistry with NHS from Azido-dPEG4-NHS dissolved in PBS (pH 7.4). After reaction for 12 h, the Azide-functionalized specimen namely the Azide/Cu-DOTA-coated specimens were then dipped into DMSO and PBS mixed solution with volume ratio of 1:4 containing 2 mg/mL of DBCO-modified AMP (i.e., (DBCO-Mal) -(Mpa) -(PEG5)-WFWKWWRRRRR) for 12 h at room temperature. In the end, the PVC functionalized by AMP and Cu-DOTA i.e., AMP@Cu-DOTA were washed by PBS and dried by N_2. The diagrammatic graph of related reaction formula for different chemical conjugations is shown in Fig. S2.

2.4. Characterization

2.4.1. Tests of amine groups on substrates before and after modification

Acid Orange (AO) II colorimetric staining method was used to determine the amine groups of the PADA-coated surfaces. Briefly, the pH of AO II aqueous solution was adjusted to 4.0 by hydrochloric acid, and then the samples were submerged in solution for 4 h. Afterwards, the samples were washed with hydrochloric acid (pH 4.0), and subsequently AO II adsorbed on the sample surfaces were eluted by NaOH aqueous solution (pH 11). Finally, the eluted solution was measured at 485 nm by using the microplate reader (μQuant, Bio-tek instruments Inc.), and the density of amine groups was calculated according to the standard curve.

High Performance Liquid Chromatography (HPLC) purification of the synthesized DBCO-AMP was performed on an Agilent HPLC system using a Kromasil 100-5C18 column (5 μm, 4.6 × 250 mm, column temperature 25 °C). Buffer A (0.1% TFA in water) and Buffer B (0.1% TFA in acetonitrile) were used as mobile phases. The flow rate was 1 mL/min with a gradient. Injection volume was 10 μL and run time was 11 min.

2.4.2. Identification of DBCO-AMP

The molecular weight of DBCO-AMP was determined by Electrospray Ionization Mass Spectrometry (ESI-MS) (Sciex API 150EX LC/MS with Agilent 1100 HPLC). Buffer: 75%ACN/24.5%H_2O/0.5%Ac; flow rate: 0.2 mL/min; run time: 1 min.

Nuclear Magnetic Resonance (NMR) spectrum (Bruker AVANCE III 400) was used to determine DBCO-AMP.

2.4.3. Characterization of the substrates before and after modification

Electron Paramagnetic Resonance (EPR) was used to analyze Cu-DOTA, the spectra were measured on a Bruker EPR EMXPlus (X-band is 9.85 GHz, the power is 0.2 mW, and field modulation is 100 kHz).

To analyze the chemical structures of the coatings, gold-plated wafer was used as the coating substrate and Reflection Absorbance Fourier transform infrared (RA-FTIR) spectrum was determined by Nicolet model 5700 instrument.

The elemental composition of the coatings was measured by X-ray photoelectron spectroscopy (XPS, XSAM200, Kratos Ltd, UK) which was supplied with a monochromatic A1 Kα (1486.6 eV) and operated at 12 kV × 15 mA with the pressure of 20×10^{-6} Pa. With the use of 300 eV pass energy, overview XPS spectra were taken between 50 and 1300 eV at 0.5 eV energy steps. The detailed spectra of peaks of interests were taken with a 0.05 eV energy step. Each sample had 15 min of total acquisition time.

2.5. Quantifications of Cu-DOTA and AMP bound to the PADA coating

The PADA film was deposited onto the AT-cut 5 MHz Au-coated quartz crystal and set in the quartz crystal microbalance with dissipation (QCM-D) equipment chamber. To make the QCM-D baseline stabilized, we injected the PBS (pH 7.4) solution with the rate of 50 μL/min continuously. Then, the WSC solution contain DOTA (0.1 mg/mL) was injected until the curve equilibrated. After that, PBS (pH 7.4) was perfused to rinse the unbound DOTA. Subsequently, the $CuCl_2{\cdot}2H_2O$ (0.1 mg/mL) were injected to realize the chelation of Cu^{2+} with DOTA for obtained Cu-DOTA-coated surface. After that, PBS was injected to remove the unchelated Cu^{2+} until obtaining the stable baseline. Before grafting of AMP, the PBS (pH 7.4) solution containing Azido-dPEG4-NHS (2 mg/mL) was supplemented to the chamber for obtaining azide-functionalized surface based carbodiimide chemistry between NHS with $–NH_2$ retained on the Cu-DOTA-coated surface. After complete reaction and rinsing by PBS, 2 mg/mL of DBCO-AMP dissolved by PBS (pH 7.4) was injected into the chamber persistently. Based on the click chemistry between DBCO and Azide, the AMP was finally immobilized on the surface. In the end, the mass of the immobilized molecular species was calculated according to the Sauerbrey equation.

2.6. Measurement of NO catalytic release

The real-time NO catalytic release from the PVC substrate (0.5 cm × 1 cm) modified by Cu-DOTA, Azide/Cu-DOTA and AMP@Cu-DOTA coatings were monitored by using a chemiluminescence NO analyzer (NOA) (Seivers 280i, Boulder, CO). 5 mL of PBS (pH 7.4) containing NO donor (10 μM GSNO, 10 μM GSH) was immitted into the run baseline. Then, the samples were immersed into the solution mentioned above and the NO would be generated from the surface of sample, which was then delivered to the NOA reaction chamber, in which NO would react with O3 and produce NO2*. With the relaxation of NO2*, the photon emitted could be measured for the computation of the catalytic NO release. In order to test the longevity of the generation of NO induced by AMP@Cu-DOTA-coated PVC, the AMP@Cu-DOTA-coated PVC was exposed to PBS containing 10 μM GSNO and 10 μM GSH (the medium was replaced every 12 h) continuously for various periods of time. After treatment by PBS for 1, 3, 5, 7, 15 and 30 days, the NO catalytic capacity of AMP@Cu-DOTA-coated PVC were performed accordingly.

2.7. Antibacterial activity in solid medium

The evaluation on anti-bacterial activities of AMP@Cu-DOTA coating was performed in accordance with ISO22196-2011. Both gram-positive *Staphylococcus epidermidis (S. epidermids),* strain American type culture collection (ATCC) 6538, and gram-negative *Escherichia coli (E. coli)*, strain ATCC 25922, were chosen for the antimicrobial tests. Firstly, bacteria were precultured in solid medium (tryptone 10 g L^{-1}, yeast extract 5 g L^{-1}, agar 15 g L^{-1} and NaCl 10 g L^{-1}, dissolved with ultrapure water) for 24 h at 37 °C and sub-cultured twice. Then freshly picked bacterial colonies (1–2 rings) with the inoculating loop and were dissolved in 0.2% liquid medium/99.8% saline (liquid medium contained yeast extract 5 g L^{-1}, tryptone 10 g L^{-1}, NaCl 10 g L^{-1} that were dissolved with ultrapure water). With the ten-fold increasing sequential dilutions, the concentration of bacteria was adjusted to $5.0 \times l0^5 \sim 10^6$ CFU mL^{-1}. After that, 200 μL of the above bacterial solution was added to the surface of sample, and covered with a film keep it wet. All samples were placed in an incubator at 37 °C for 24 h. Finally, bacteria on the surface were rinsed and dissolved in 20 mL saline solution, and 200 μL of the above bacterial solution was added to the solid medium at 37 °C. After culture for 24 h, the colonies on the solid medium were counted.

2.8. Antibacterial activity in solution

After preculture in solid medium, we transferred fresh bacterial colonies (1–2 rings) to liquid medium and cultivated them for 24 h and diluted for 10^6 times. Then, all samples were placed in a 24-well plate. After that, each sample was immersed into 200 μL diluted bacterial solution (10^6 CFU mL^{-1}) at 37 °C. After cultivation for 12 h, 800 μL liquid medium was supplemented to the samples and cultured for another 12 h. Finally, 200 μL solution was removed to measure the optical density (OD) value at 600 nm.

2.9. Hemolysis rate

All the samples were placed into centrifuge tubes with 9.8 mL saline respectively and the equal amount of ultrapure water and saline without sample were set as the positive and negative control. Then, the fresh human blood (2 mL) with trisodium citrate dihydrate (109 mmol/L) was diluted with saline (2.5 mL), and 200 μL of the diluted blood was added into the tube to incubate at 37 °C for 1 h. Finally, all the blood samples were centrifuged at 1500g for 5 min to measure the released hemoglobin. And the hemolysis ratio was measure according to ASTM F756-08 [23].

2.10. Fibrinogen adsorption and activation

The fresh human whole blood used in this study was legally acquired from the Chengdu central blood station following the ethics standards and all volunteers did not take medicine in the recent 2 weeks. The blood was anti-coagulated with tri-sodium citrate (4% wt) in a volumetric ratio of 9:1. The platelet poor plasma (PPP) and platelet rich plasma (PRP) were obtained by centrifugation of fresh human whole blood under 3000 rpm and 1500 rpm for 15 min respectively.

Fibrinogen adsorption was tested by adding 50 μL of PPP with or without NO donor (10 μM GSNO, 10 μM GSH) onto samples. After incubation for 2 h at 37 °C, the sample was washed with PBS, and then 20 μL of horse radish peroxidase (HRP) labeled sheep polyclonal antibody anti-human fibrinogen (Sigma-Aldrich) was introduced and incubated for 60 min. Subsequently, chromogenic substrate 3,3′,5,5′-tetramethylbenzidine solution (TMB, 100 μL) was added. After 10 min, the color reaction was terminated by introducing acid solution, while measurement at 405 nm (absorbance) was performed.

In the case of fibrinogen activation, the sample was firstly incubated with PPP for 120 min. After washing by PBS, it was continuously incubated with mouse anti-human γ-fibrinogen monoclonal antibody (20 μL) at 37 °C for 1 h. Subsequently, the sample was washed by PBS, and then reacted with HRP labeled sheep anti-mouse polyclonal antibody (20 μL). Afterwards, TMB solution (100 μL) was added. After reaction for 10 min, the above mixed solution was measured at 405 nm.

2.11. cGMP synthesized by platelets

The expression level of cGMP was measured by ELISA. In brief, 1 mL of PRP with or without NO donor (10 μM GSNO, 10 μM GSH) was dropped on each specimen. After incubation for 30 min, 100 μL triton-X solution (10%) was added and sonicated, and then the obtained solution was centrifugated at 1200 rcf for 8min to gain the supernatant for ELISA test [24].

2.12. Adhesion and activation of platelets

The experiments were carried out within 12 h after the blood donation. In consideration of the chemical instability of endogenous donor of RSNO in PRP, an extra NO donor consisting of 10 μM GSNO and 10 μM GSH was added to act as a comparison analysis. 1 mL of PRP, with or without NO donor, was dropped on the surface of each specimen and incubated for 2 h at 37 °C in humidified air. After that, the samples were rinsed with 0.9% NaCl solution and fixed with 2.5% glutaraldehyde overnight. With further dehydration and dealcoholizing, the surfaces of samples were sputtered with gold and examined by scanning electron

microscope (SEM, Quanta 200, FEI, Netherlands).

2.13. Anti-thrombogenicity test by ex-vivo blood circulation

All the studies followed the animal use protocol of the China Council on Animal Care and Southwest Jiaotong University, obeying the ethical rules for experimental animals. Eight adult New Zealand white rabbits (2.5–3.5 kg) were used for this experiment. General anesthesia was carried out to all experimental animals. The left carotid artery and the right jugular vein of the rabbits were isolated and connected with the arteriovenous (AV) extracorporeal circuit (ECC) by cannula. The PVC tubes before and after functionalization by AMP@Cu-DOTA were connected to the ECC tightly. The blood flow began by loosening the arterial and venous sides of the ECC. After 3 h of blood circulation, the experiments were stopped and the blood flow rates of the circuits were measured [25]. The cross section of the experimental tubing and the weight of the residual thrombus on the samples were obtained to evaluate the anti-coagulant effect of the specimens. Afterwards, the samples were washed by PBS (pH 7.4) and fixed in 2.5% glutaraldehyde solution overnight. After dehydration and critical point drying, the samples were observed by SEM (As shown in Fig. 6e).

3. Results and discussion

3.1. Synergistic co-grafting of Cu-DOTA and AMP on PVC

3.1.1. Identification of DBCO-AMP and Cu-DOTA

The DBCO-AMP was designed and fabricated by standard Fmoc mediated solid-phase peptide synthesis (Fig. 2a) [26]. ESI-MS and NMR were used for confirming the success of DBCO-AMP synthesis. ESI-MS analysis indicated that the monoisotopic mass of $[M+4H]^{4+}$ and $[M+3H]^{3+}$ at 654 and 871 Da, respectively (Fig. 2b) was in line with its theoretical molecular weight of 2612.0 Da. The spectrum of ^{1}H NMR revealed the presence of typical diagnostic peaks specific to the DBCO-AMP (Fig. 2c). Taken together, these results demonstrated the successful synthesis of DBCO-AMP. The spectra of EPR showed the successful synthesis of Cu-DOTA coordination complex, as evidenced by the presence of Cu-DOTA signal at 267 mT (Fig. 2d).

3.1.2. Characterization of coated surface

Since the consumption of amine groups can reflect the graft of molecular, the remaining amine groups on the different surface as shown in Fig. S1. The high density of 13.13 ± 0.31 nmol/cm^2 of the amine groups on the PADA coating indicated the successful preparation of the amine-bearing surface. Meanwhile, with the grafting of Cu-DOTA and Azido-dPEG4-NHS in sequence, the densities of the residual amine groups on the surface were 6.41 ± 0.73 nmol/cm^2 and 0.01 ± 0.03 nmol/cm^2 respectively, implying the success of the molecular conjugation. To

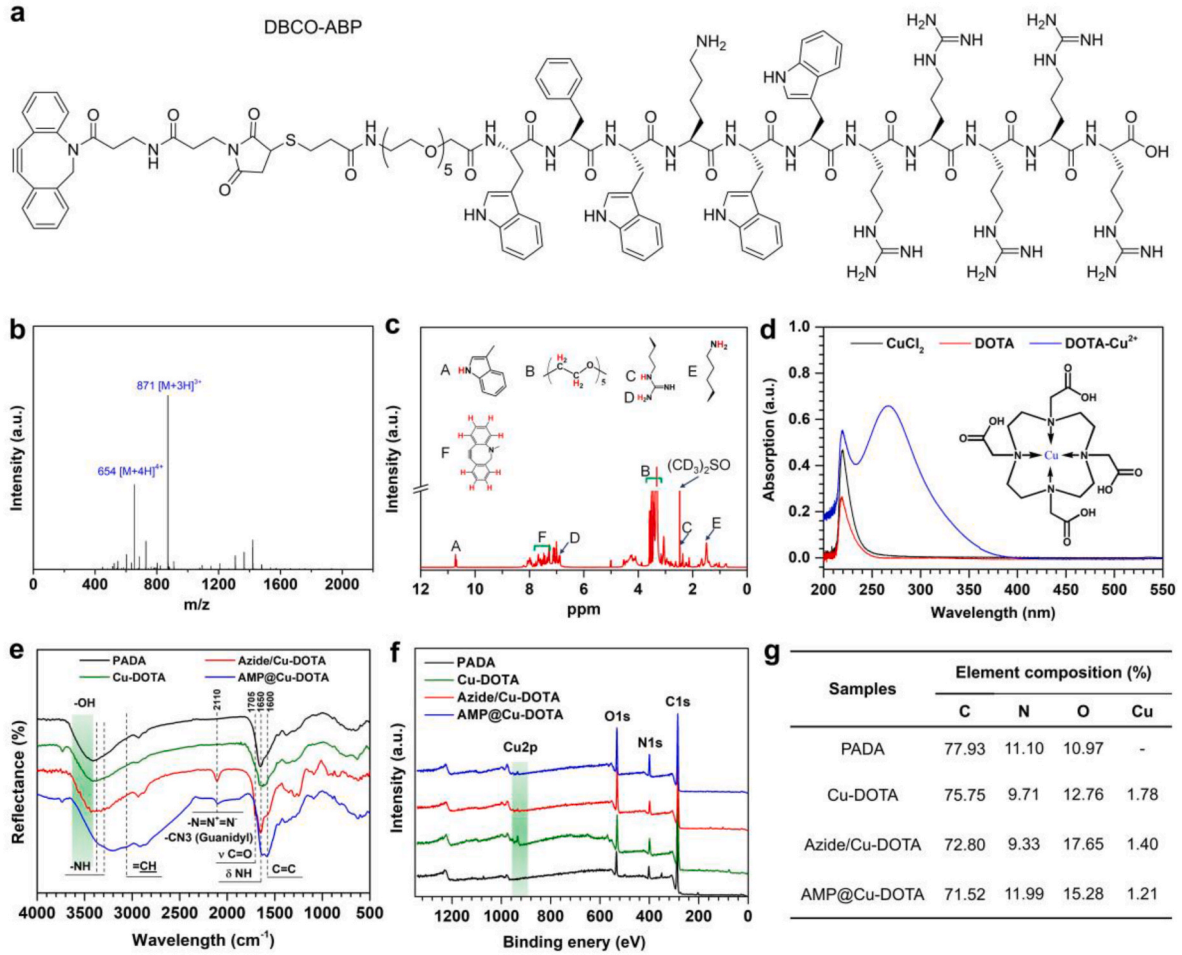

g

Samples	Element composition (%)			
	C	N	O	Cu
PADA	77.93	11.10	10.97	-
Cu-DOTA	75.75	9.71	12.76	1.78
Azide/Cu-DOTA	72.80	9.33	17.65	1.40
AMP@Cu-DOTA	71.52	11.99	15.28	1.21

Fig. 2. (a) Structural formula of the DBCO-modified antibacterial peptide (DBCO-AMP). (b) ESI mass spectrum of the DBCO-AMP. (c) NMR spectrum of the DBCO-AMP. (d). UV spectra of copper chloride, DOTA and Cu-DOTA solution. (e) RA-FTIR spectra, (f) XPS wide-scan survey and (g) the corresponding elemental compositions on the surfaces of PADA, Cu-DOTA, Azide/Cu-DOTA and AMP@Cu-DOTA.

demonstrate the successful co-grafting of Cu-DOTA and DBCO-AMP on the amine-bearing PADA-coated surface, RA-FTIR and XPS were performed. As shown in Fig. 2e, the conjugation of Cu-DOTA on the PADA led to the presence of a new peak at 1705 cm^{-1} assigned to the Amide I (O═C–NH), and reinforcement in the band around 1640-1600 cm^{-1} corresponding to the Amide II (O═C–NH) in the spectrum of Cu-DOTA, indicating the amination reaction between –COOH of Cu-DOTA and $–NH_2$ provided by PADA coating. The presence of peak at 2110 assigned to the $–N═N^{+}═N^{-}$ and further reinforcement in the Amide I and Amide II bands in the spectrum of Azide/Cu-DOTA compared with the spectrum of Cu-DOTA strongly confirmed the effective azidation to the Cu-DOTA. The introduction of Azide to the Cu-DOTA surface provided the anchoring site with functional groups for further immobilization of DBCO-AMP. The spectrum of AMP/Cu-DOTA revealed the presence of some new peaks at 3060 (=CH stretching), 2100 (Guanidyl stretching), and 1600 cm^{-1} (C═C stretching) that were specific to the AMP, indicating the successful conjugation of AMP. The significant variations in the surface chemical compositions among the groups of PADA (Fig. 2f and g), Cu-DOTA, Azide/Cu-DOTA and AMP@Cu-DOTA further confirmed the effective immobilization of Cu-DOTA and AMP. 1.78% of Cu content was determined on the surface, implying the successful creation of the NO-generating surface. It was also found that the tethering of AMP led to 30% of shielding effects approximately on NO catalytic active site of Cu (Fig. 2g), as evidenced by the remarkable reduction in Cu content.

3.1.3. *Quantitative measurement of Cu-DOTA and AMP conjugation and NO catalytic capacity*

To quantitatively measure the amount of Cu-DOTA and AMP bound to the PADA coating, QCM-D analysis was carried out. The DOTA was pumped into the system continuously until the curve equilibrated, and the amount of DOTA bound to the surface was 319.08 ng/cm^2 after rinsing with PBS as shown in Fig. 3a. Then, the $CuCl_2$ were injected accordingly and the Cu-DOTA was harvested on the PADA coating (339.94 ng/cm^2). After that, with the injection of Azido-dPEG4-NHS, the curve rose gradually providing the evidence for the click chemistry of peptide. Finally, with perfusion of AMP solution, the amount of AMP bound to the surface was 1523.07 ng/cm^2 after the sufficient wash by

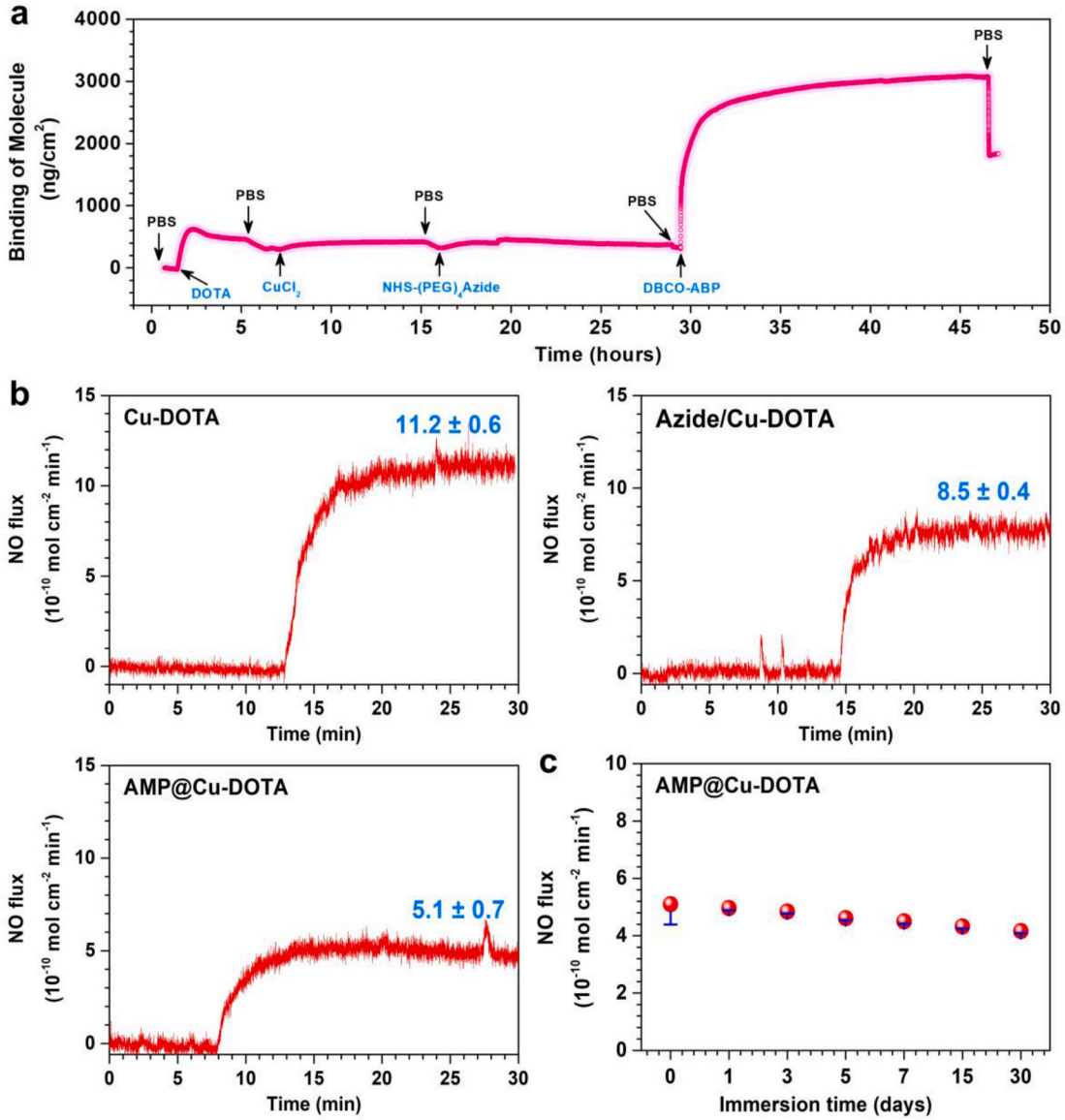

Fig. 3. a) Real-time monitoring of DOTA, Cu^{2+}, NHS-$(PEG)_4$Azide, DBCO-AMP grafting process on a PADA-coated chip determined by QCM. b) Effects of NHS-Azide and DBCO-AMP grafting on NO generation. c) Retention of NO catalytic capacity of AMP@Cu-DOTA coating after continuous treatment by PBS containing NO donor (10 μM GSNO, 10 μM GSH). Data are presented as mean ± SD (n = 4).

PBS revealing the successful grafting of functional molecules.

In our design, the Cu^{2+} chelated in DOTA decomposes RSNO into NO to prevent material-induced thrombosis. Thus, the release of NO was measured to evaluate the successful design of the AMP@Cu-DOTA. To test the NO catalytic activity of AMP@Cu-DOTA-coated PVC, the chemiluminescence assay of real-time quantitative analysis was used to evaluate the generation of NO in NO donor solution consisting of 10 μM GSNO and 10 μM GSH (pH 7.4). The NO production patterns as shown in Fig. 3b illustrated a stable persistent release of NO from Cu-DOTA-coated PVC ($11.2 \pm 0.6 \times 10^{-10}$ mol cm^{-2} min^{-1}), revealing the successful biofunctionalization of local delivery of NO. Furtherly, the release rate of NO catalyzed by the samples of Azide/Cu-DOTA and AMP@Cu-DOTA are $8.5 \pm 0.4 \times 10^{-10}$ mol cm^{-2} min^{-1} and $5.1 \pm 0.7 \times 10^{-10}$ mol cm^{-2} min^{-1}. Meanwhile, the reduced release of NO in the Adize/Cu-DOTA and AMP@Cu-DOTA groups was significant because it implied the successful immobilization of both molecules. To be medically relevant, the biofunctionalized coating must exhibit persisting release of NO. The evaluation of the catalytic NO reflected that the AMP@Cu-DOTA coating still showed a steady NO release rate of $4.2 \pm 0.1 \times 10^{-10}$ mol cm^{-2} min^{-1} after immersion for 30 days maintaining ~83.9% compared with the initial NO generation (Fig. 3c).

3.2. Anti-bacterial properties

For the indwelling medical devices or extracorporeal circuits, bacterial infection is a crucial complication after implantation. Hence, antibacterial functionalization of surface becomes essential for these devices. To test the antibacterial properties of the AMP@Cu-DOTA coating, we examined surface sterilization of gram-negative *E. coli* and gram-positive *S. epidermids* in solid culture and liquid culture. We found that in the solid media, the PADA coating endowed PVC pattern with ability to resist *E. coli* (46.6 ± 7.0%) and *S. epidermids* (45.0 ± 7.0%) which might contribute to the positively charged amine groups introduced on the surface. Meanwhile, there was a slight increase of the antibacterial rate in Cu-DOTA coated PVC compared with the PADA group. According to the NO release rate of Cu-DOTA and Azide/Cu-DOTA coating, the reported values were lower than the antibacterial requirement of NO reported elsewhere (approximately 1 ppm). Nonetheless, the effective antibacterial property might be owing to the sterilization ability of Cu^{2+} from Cu-DOTA. In addition, we have noted that the surface functionalization by AMP@Cu-DOTA on the PADA-coated PVC showed excellent antibacterial rates of 95.2 ± 5.6 and 96.1 ± 8.6 in *E. coli* and *S. epidermids* respectively, suggesting that the excellent bacterial activity of AMP in the biofunctionalized surface was intactly maintained by click chemistry (Fig. 4b and c). Subsequently, all the samples were immersed in bacterium suspensions, which were used to evaluate the potent bacterial inhibition of AMP@Cu-DOTA coatings in liquid media. After measuring the optical density of bacterial solutions incubated with different groups, the similar results were observed. As shown in Fig. 4d and e, 96.0 ± 7.0% of *E. coli* and 96.4 ± 7.7% of *S. epidermids* could be killed by AMP@Cu-DOTA coating modified PVC, furtherly demonstrating the successful design of AMP@Cu-DOTA coating to endow the PVC pattern with potent antibacterial capabilities.

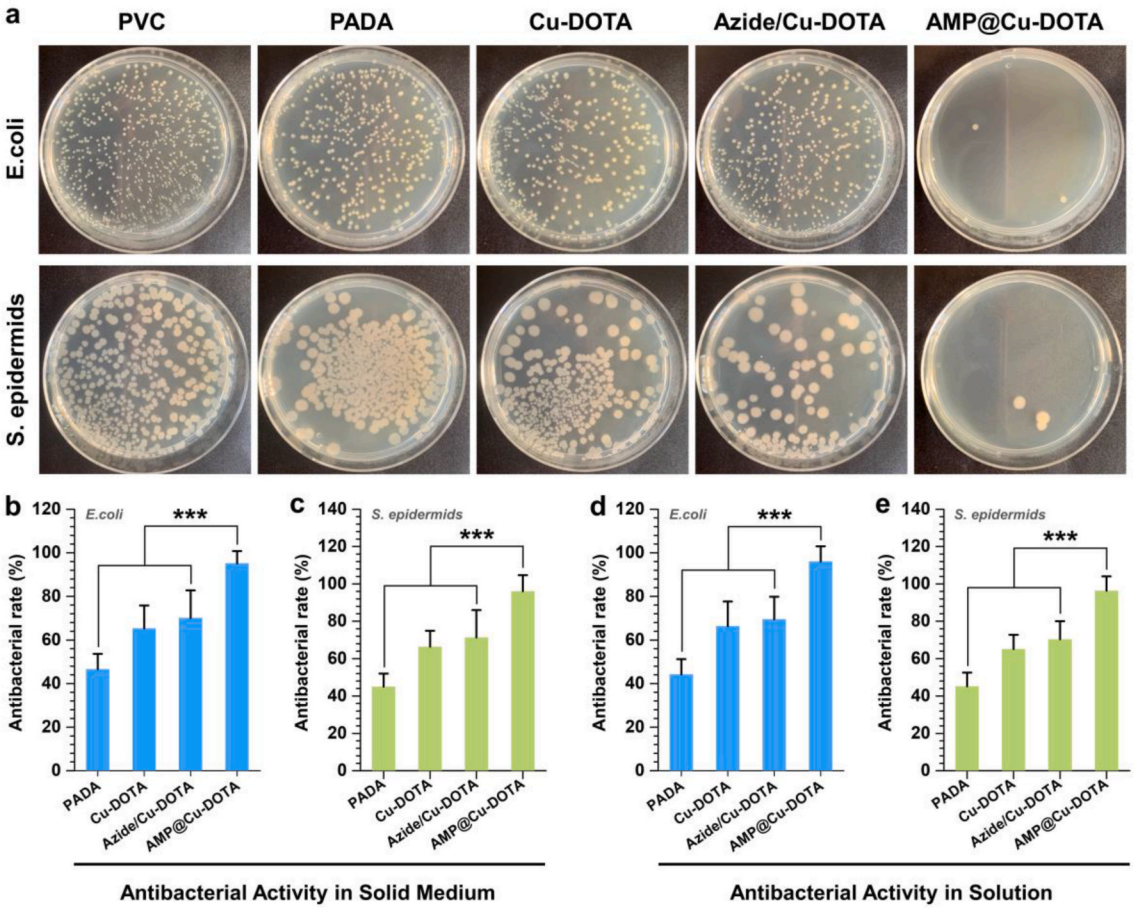

Fig. 4. Representative colonization of *E. coli* and *S. epidermids* on the PVC substrates before and after coating with PADA and Cu-DOTA, Azide/Cu-DOTA and AMP@Cu-DOTA. a) Colonization photographs of *E. coli* and *S. epidermids*. The antibacterial rate of different surfaces against *E. coli* (b) and *S. epidermids* (c) performed by Solid Medium method. The antibacterial rate of different surfaces against *E. coli* (d) and *S. epidermids* (e) performed by solution method. Data are presented as mean ± SD (n = 4) and analyzed by one-way ANOVA (***$p < 0.001$).

3.3. In vitro hemolysis and anticoagulation properties

As a new foreign blood-contacting material, hemolysis ratio (HR) is one of the most crucial factors to determine whether it can be applied in clinic. Therefore, the HR of the PADA coating before and after further secondary modification by Cu-DOTA and AMP was evaluated. As shown in Fig. 5a, the hemolysis ratios of the PADA, Cu-DOTA, Azide/Cu-DOTA and AMP@Cu-DOTA are within 1%, which is far below the internationally accepted standard value of 5% [27], implying the potential feasibility of the PADA and its derivative coatings applied in blood-contacting devices. For a blood-contacting device, good blood compatibility involves not only acceptable HR, but also low adsorption/activation of fibrinogen and adhesion/activation platelets. The results of fibrinogen revealed that the modification by PADA did not lead to significant effects on both adsorption (Fig. 5b) and activation (Fig. 5c) of fibrinogen. Of special importance is that the grafting of Cu-DOTA (i.e., Cu-DOTA) resulted in a remarkable reduction in fibrinogen adsorption and activation as compared to the PADA, which might be ascribed to the consumption of the surface positively charged amine groups of PADA during the amination between amine groups and carboxyl groups of Cu-DOTA [28]. We also noted that the subsequent azidation and further conjugation of AMP to the Cu-DOTA did not influence the behavior of fibrinogen on its surface, as evidenced by the same level adsorption and activation of fibrinogen. It is well known that the inhibitory effect of NO on platelet is based on its ability to up-regulate the expression of cGMP [29]. To confirm the efficiency of NO generated by Cu-DOTA on promoting the expression of cGMP of platelets, cGMP analysis was performed. As expected, the Cu-DOTA promoted the synthesis of cGMP of platelets (Fig. 5 d). Moreover, we found that the reduction of NO induced by Azide/Cu-DOTA and AMP@Cu-DOTA (Fig. 3b) led to the decrease in the cGMP expression. Subsequently, the effects of NO on platelet adhesion and activation were further carried out. SEM analysis revealed that most of the platelets adhered on both PVC and PADA showed activated state accompanied with pseudopodium (Fig. 3e). For the PADA, some platelets were fully spread due to the presence of a large number of positively charged amine groups [28]. In contrast, the release of NO induced by Cu-DOTA significantly reduced adhesion and activation of platelets from ~20% (Fig. 3f) and ~80% (Fig. 3g) of PVC to less than 4% and 20% respectively. Although the production of NO induced by Azide/Cu-DOTA and AMP@Cu-DOTA is lower than that of Cu-DOTA,

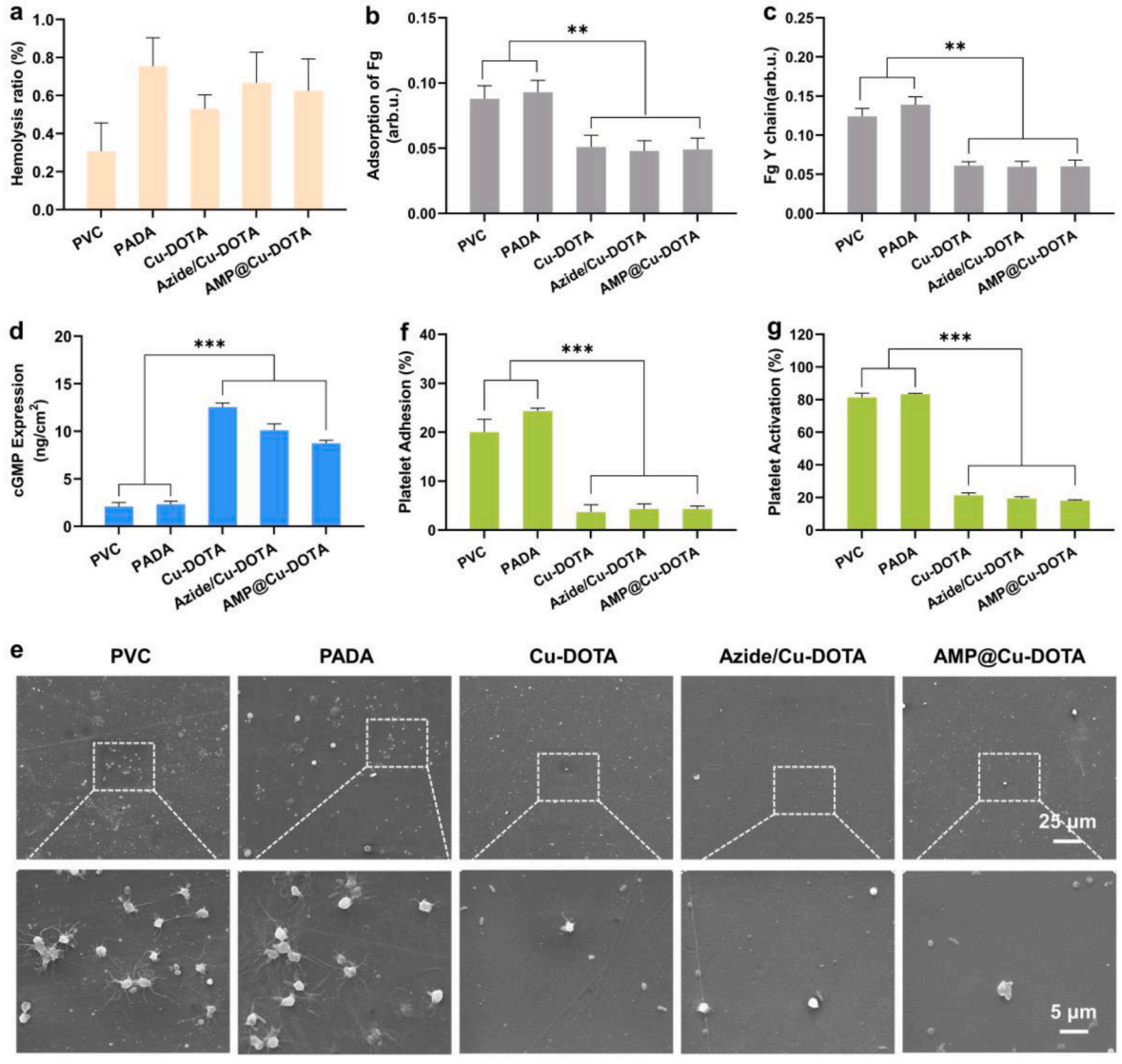

Fig. 5. Hemocompatibility test *in vitro*. a) Hemolysis ratios, b) fibrinogen adsorption, c) fibrinogen activation of PVC substrates before and after functionalization by PADA and Cu-DOTA, Azide/Cu-DOTA and AMP@Cu-DOTA coatings. d) cGMP expression of platelets on different surfaces after 2 h. e) Representative SEM images of platelets adhered on different surfaces. f) Adhesion and g) activation of platelets incubated with different surfaces for 2 h. Data presented as mean ± SD and analyzed using a one-way ANOVA, $^{**}p < 0.01$, $^{***}p < 0.001$.

they still showed the substantial inhibitory effects on both adhesion and activation of platelets. Taken together these results indicated that AMP@Cu-DOTA coating reduces fibrinogen adsorption and activation, and suppresses both adhesion and activation of platelets, hence confirming its improved anti-thrombogenicity *in vitro*.

3.4. Ex-vivo anti-thrombogenicity

To further attest the ability of AMP@Cu-DOTA-coated PVC to prevent the formation of thrombosis, *ex vivo* circulation antithrombogenic evaluation was performed. Here, an arteriovenous (AV) shunt model was used for the *ex vivo* antithrombogenic test, as reported previously [22]. As shown in Fig. 6a, the commercially available PVC tubing before and after functionalization by AMP@Cu-DOTA were assembled into an extracorporeal circuit (ECC). The anti-thrombogenic properties of AMP@Cu-DOTA coating were evaluated by analysis of occlusive rate, thrombosis and blood flow rate of circuits after 3 h of *ex vivo* circulation without any anti-coagulant treatment to blood in the New Zealand white rabbit AV shunt model.

It was clear that after 3 h of *ex vivo* circulation, the bare PVC circuit showed the almost complete occlusion (Fig. 6b) with 91.2 ± 7.6% of occlusive rate (Fig. 6c), whereas the AMP@Cu-DOTA-modified circuit significantly reduced the occlusive rate to 12.3 ± 1.4%. The statistical analysis of thrombosis formed in the circuits revealed that coating PVC tubing internal surface with AMP@Cu-DOTA reduced the thrombus by 10-fold, as compared to the control PVC circuit (Fig. 6d). Further analysis by SEM confirmed the efficiency of AMP@Cu-DOTA coating to percent the formation of thrombi on its coated surface. On the internal surface the unmodified PVC tubing, very severe clots with cross-linked dense fibrillar networks of polymerized fibrin, activated platelets and red blood cells were clearly observed (Fig. 6e).

On the other hand, surface coated with AMP@Cu-DOTA effectively prevented activation of platelets, polymerization of fibrinogen, and hence the formation of thrombi. There were only few of platelets remained in a resting, nonactivated state found on the AMP@Cu-DOTA-coated surface. In the end, the AMP@Cu-DOTA-modified circuit remained 94.5 ± 7.6% of blood flow rate after 3 h of circulation, which is much higher than that of control circuit with blood flow rate of only 18.2 ± 2.1% (Fig. 6f).

Taken together with the anti-bacterial results, the stepwise synergistic modification strategy by using anticoagulant NO and antibacterial peptide AMP imparted the PVC with dual functions to combat biofouling and thrombosis, indicating the promising application in extracorporeal circuits and indwelling medical devices.

4. Conclusion

In summary, we developed a stepwise conjugating strategy for constructing anti-coagulant and anti-bacterial surface on the semi-implanted blood-contacting tubing. To realize dual functions capable of combating thrombosis and anti-fouling, an anti-bacterial peptide and a NO-generating species were sequentially conjugated on the tubing surface through carbodiimide and click chemistry respectively. The synergistic actions of NO catalytic generation and anti-bacterial peptide resulted in significant inhibition both in adhesion and activation of platelets, and in bacteria growth *in vitro*. Moreover, such dual-functional tubing also effectively prevented the formation of thrombosis *ex vivo*. Overall, this work might provide a new strategy not only for tailoring

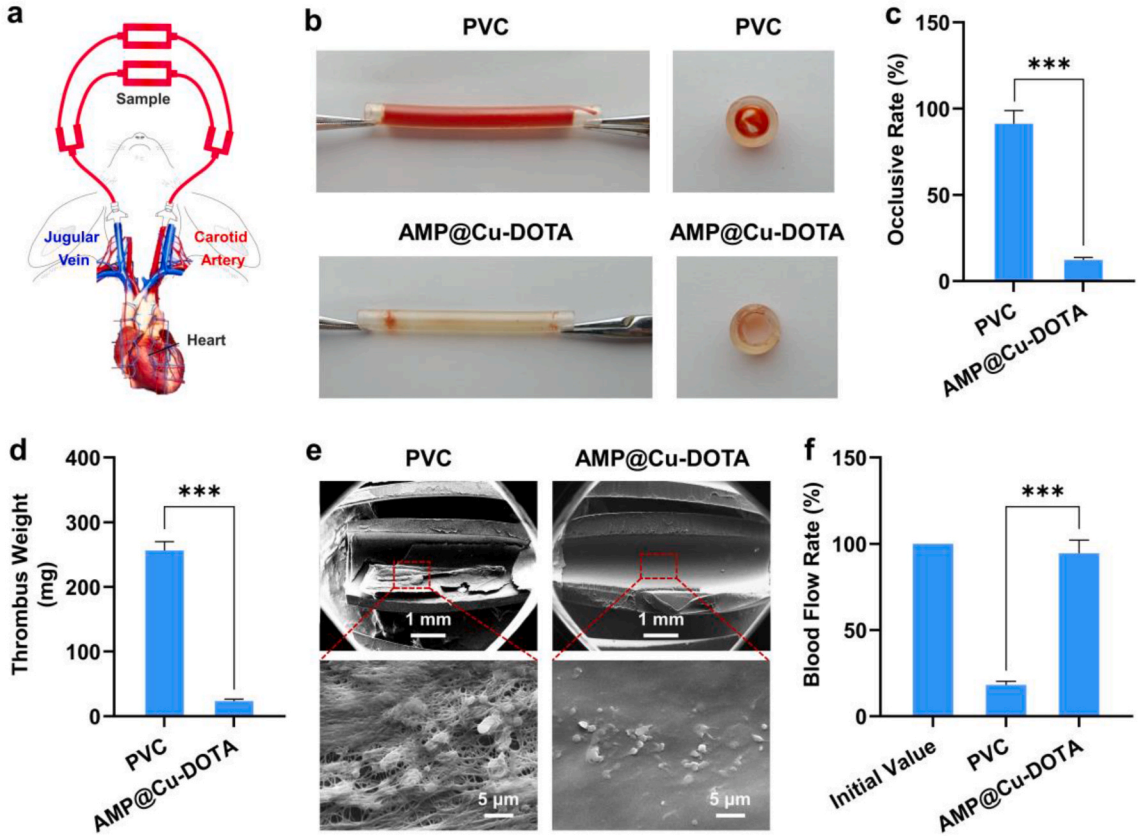

Fig. 6. Scheme of the New Zealand white rabbit AV shunt model exhibiting placement of the cannula in the carotid artery and jugular vein connected by the PVC tubing before and after coating with AMP@Cu-DOTA. b) Photographs of the tubing (Left) and cross section of circuits (Right) after circulation for 3 h. c) Occlusive rate of the circuits before and after modification by AMP@Cu-DOTA coating. d) Weight of thrombus formed in the unmodified- and AMP@Cu-DOTA-modified circuits. e) SEM images of the tubing luminal sides. f) Blood flow rate of circuits at the end of circulation experiments. Data are presented as mean ± SD (n = 4) and analyzed by one-way ANOVA (***$p < 0.001$).

surface multi-functionalities, but also a promising solution for addressing the clinical complications of extracorporeal circuits and indwelling medical devices associated with thrombosis and infection.

CRediT authorship contribution statement

Han Yu: Conceptualization, Methodology, Writing - review & editing, Writing - original draft. **Shaoxing Yu:** Conceptualization, Methodology, Writing - original draft. **Hua Qiu:** Conceptualization, Methodology, Writing - original draft. **Peng Gao:** Conceptualization, Methodology, Writing - original draft. **Yingzhong Chen:** Conceptualization, Methodology, Writing - original draft. **Xin Zhao:** Conceptualization, Methodology, Writing - review & editing, Writing - original draft. **Qiufen Tu:** Conceptualization, Methodology, Writing - original draft. **Minggang Zhou:** Conceptualization, Methodology, Supervision, Writing - original draft. **Lin Cai:** Conceptualization, Methodology, Writing - original draft. **Nan Huang:** Conceptualization, Methodology, Writing - original draft. **Kaiqin Xiong:** Conceptualization, Methodology, Supervision, Writing - original draft. **Zhilu Yang:** Conceptualization, Methodology, Supervision, Writing - review & editing, Writing - original draft.

Declaration of competing interest

The authors declare that they have no known competing financial interests or personal relationships that could have appeared to influence the work reported in this paper.

Acknowledgments

This work was supported by the National Natural Science Foundation of China (Project 82072072), National Key Research and Development Program of China (2017YFB0702504), International Cooperation Project by Science and Technology Department of Sichuan Province (2019YFH0103), the Fundamental Research Funds for the Central Universities (2682020ZT76) and the Innovation and Technology Fund (ITS/065/19) from the Innovation and Technology Commission of Hong Kong. We would like to thank Analytical and Testing Center of Southwest Jiaotong University for scanning electron microscope detection.

Appendix A. Supplementary data

Supplementary data to this article can be found online at https://doi.org/10.1016/j.bioactmat.2020.11.011.

References

[1] I.H. Jaffer, J.I. Weitz, The blood compatibility challenge. Part 1: blood-contacting medical devices: the scope of the problem, Acta Biomater. 94 (2019) 2–10.
[2] L. Nisa, K. Nicoucar, R. Giger, Major bleeding of the upper aerodigestive tract due to oral anticoagulant/antibiotic interactions, Eur. Ann. Otorhinolaryngol. Head Neck Dis. 130 (3) (2013) 153–156.
[3] T.E. Warkentin, M.N. Levine, J. Hirsh, P. Horsewood, R.S. Roberts, M. Gent, J. G. Kelton, Heparin-induced thrombocytopenia in patients treated with low-molecular-weight heparin or unfractionated heparin, N. Engl. J. Med. 332 (20) (1995) 1330–1335.
[4] A. Kumar, H.P. Schweizer, Bacterial resistance to antibiotics: active efflux and reduced uptake, Adv. Drug Deliv. Rev. 57 (10) (2005) 1486–1513.
[5] C. Nwokolo, L. Byrne, K.J. Misch, Toxic epidermal necrolysis occurring during treatment with trimethoprim alone, Br. Med. J. 296 (6627) (1988) 970.
[6] J. Badger, Long peripheral catheters for deep arm vein venous access: a systematic review of complications, Heart Lung 48 (3) (2019) 222–225.
[7] P.J. Pronovost, C.A. Goeschel, E. Colantuoni, S. Watson, L.H. Lubomski, S. M. Berenholtz, D.A. Thompson, D.J. Sinopoli, S. Cosgrove, J.B. Sexton, J. A. Marsteller, R.C. Hyzy, R. Welsh, P. Posa, K. Schumacher, D. Needham, Sustaining reductions in catheter related bloodstream infections in Michigan intensive care units: observational study, BMJ 340 (feb04 1) (2010) c309.
[8] N. Ajdari, C. Vyas, S.L. Bogan, B.A. Lwaleed, B.G. Cousins, Gold nanoparticle interactions in human blood: a model evaluation, Nanomed.Nanotechnol. 13 (4) (2017) 1531–1542.
[9] F. Wu, T.T. Xu, G.Y. Zhao, S.S. Meng, M.M. Wan, B. Chi, C. Mao, J. Shen, Mesoporous silica nanoparticles-encapsulated agarose and heparin as anticoagulant and resisting bacterial adhesion coating for biomedical silicone, Langmuir 33 (21) (2017) 5245–5252.
[10] S.K. Hendricks, C. Kwok, M. Shen, T.A. Horbett, B.D. Ratner, J.D. Bryers, Plasma-deposited membranes for controlled release of antibiotic to prevent bacterial adhesion and biofilm formation, J. Biomed. Mater. Res.: Off. J. Soc. Biomater. Jap. Soc. Biomater. Austr. Soc. Biomater. kor. Soc. Biomater. 50 (2) (2000) 160–170.
[11] M.C. Munisso, T. Yamaoka, Peptide with endothelial cell affinity and antiplatelet adhesion property to improve hemocompatibility of blood-contacting biomaterials, Peptide Sci. 111 (5) (2019), e24114.
[12] W.L. Hynes, S.L. Walton, Hyaluronidases of gram-positive bacteria, FEMS Microbiol. Lett. 183 (2) (2000) 201–207.
[13] T. Tischer, T.K. Claus, M. Bruns, V. Trouillet, K. Linkert, C. Rodriguez-Emmenegger, A.S. Goldmann, S. Perrier, H.G. Borner, C. Barner-Kowollik, Spatially controlled photochemical peptide and polymer conjugation on biosurfaces, Biomacromolecules 14 (12) (2013) 4340–4350.
[14] V. Kutay, T. Noyan, S. Ozcan, Y. Melek, H. Ekim, C. Yakut, Biocompatibility of heparin-coated cardiopulmonary bypass circuits in coronary patients with left ventricular dysfunction is superior to PMEA-coated circuits, J. Card. Surg. 21 (6) (2010) 572–577.
[15] D. Reser, B. Seifert, M. Klein, T. Dreizler, P. Hasenclever, V. Falk, C. Starck, Retrospective analysis of outcome data with regards to the use of Phisio (R)-, Bioline (R)- or Softline (R)-coated cardiopulmonary bypass circuits in cardiac surgery, Perfusion-Uk 27 (6) (2012) 530–534.
[16] E.J. Schiffrin, F. Rochat, H. Link-Amster, J.M. Aeschlimann, A. Donnet-Hughes, Immunomodulation of human blood cells following the ingestion of lactic acid bacteria, J. Dairy Sci. 78 (3) (1995) 491–497.
[17] S.J. Peacock, T.J. Foster, B.J. Cameron, A.R. Berendt, Bacterial fibronectin-binding proteins and endothelial cell surface fibronectin mediate adherence of Staphylococcus aureus to resting human endothelial cells, Microbiology 145 (12) (1999) 3477–3486. Pt 12.
[18] T. Ganz, J. Weiss, Antimicrobial peptides of phagocytes and epithelia, Semin. Hematol. 34 (4) (1997) 343–354.
[19] M. Zasloff, Antimicrobial peptides of multicellular organisms, Nature 415 (6870) (2002) 389–395.
[20] M. Zasloff, Antimicrobial peptides of multicellular organisms: my perspective, Adv. Exp. Med. Biol. 1117 (2019) 3–6.
[21] A. Gries, C. Bode, K. Peter, A. Herr, H. Bohrer, J. Motsch, E. Martin, Inhaled nitric oxide inhibits human platelet aggregation, P-selectin expression, and fibrinogen binding in vitro and in vivo, Circulation 97 (15) (1998) 1481–1487.
[22] Q. Tu, X. Shen, Y. Liu, Q. Zhang, X. Zhao, M.F. Maitz, T. Liu, H. Qiu, J. Wang, N. Huang, Z. Yang, A facile metal–phenolic–amine strategy for dual-functionalization of blood-contacting devices with antibacterial and anticoagulant properties, Mater. Chem. Front. 3 (2) (2019) 265–275.
[23] Standard Recommended Practice for the Assessment of the Hemolytic Properties of Materials, Book of Standards, ASTM International, West Conshohocken, PA, USA, 2008, ASTM-F756-08.
[24] Z. Yang, Y. Yang, K. Xiong, X. Li, P. Qi, Q. Tu, F. Jing, Y. Weng, J. Wang, N. Huang, Nitric oxide producing coating mimicking endothelium function for multifunctional vascular stents, Biomaterials 63 (2015) 80–92.
[25] P. Gao, H. Qiu, K. Xiong, X. Li, Q. Tu, H. Wang, N. Lyu, X. Chen, N. Huang, Z. Yang, Metal-catechol-(amine) networks for surface synergistic catalytic modification: therapeutic gas generation and biomolecule grafting, Biomaterials 248 (2020) 119981.
[26] G. Pan, S. Sun, W. Zhang, R. Zhao, W. Cui, F. He, L. Huang, S.H. Lee, K.J. Shea, Q. Shi, H. Yang, Biomimetic design of mussel-derived bioactive peptides for dual-functionalization of titanium-based biomaterials, J. Am. Chem. Soc. 138 (45) (2016) 15078–15086.
[27] L. Li, M. Tu, S. Mou, C. Zhou, Preparation and blood compatibility of polysiloxane/liquid-crystal composite membranes, Biomaterials 22 (19) (2001) 2595–2599.
[28] Z. Yang, J. Wang, R. Luo, M.F. Maitz, F. Jing, H. Sun, N. Huang, The covalent immobilization of heparin to pulsed-plasma polymeric allylamine films on 316L stainless steel and the resulting effects on hemocompatibility, Biomaterials 31 (8) (2010) 2072–2083.
[29] K.S. Bohl, J.L. West, Nitric oxide-generating polymers reduce platelet adhesion and smooth muscle cell proliferation, Biomaterials 21 (22) (2000) 2273–2278.